On the relevance of aerosols to snow cover variability over High Mountain Asia

Chayan Roychoudhury[1#], Cenlin He[2], Rajesh Kumar[2], John M. McKinnon[1], Avelino F. Arellano Jr.[1]

[1]Department of Hydrology and Atmospheric Sciences, University of Arizona, Tucson, AZ, USA

[2]Research Applications Laboratory, National Center for Atmospheric Research, Boulder, CO, USA

Key Points

1. Interactions between aerosols and meteorology are significant during late snowmelt (June-July) over low snow-covered regions in HMA.
2. Species related interactions drive the seasonal variability of the overall relative importance.
3. Carbonaceous aerosols are more relevant than mineral dust during late snowmelt.

Abstract

While meteorology and aerosols are identified as key drivers of snow cover variability in High Mountain Asia (HMA), complex non-linear interactions between them are not adequately quantified. Here, we attempt to unravel these interactions through a simple relative importance (RI) analysis of meteorological and aerosol variables from ERA5/CAMS-EAC4 reanalysis against satellite-derived snow cover from MODIS across 2003-2018. Our results show a statistically significant 7% rise in the RI of aerosol-meteorology interactions (AMI) in modulating snow cover during late snowmelt season (June-July), notably over low snow-covered (LSC) regions. Sensitivity tests further reveal that the importance of meteorological interactions with individual aerosol species are more prominent than total aerosols over LSC regions. We find that the RI of AMI for LSC regions is clearly dominated by carbonaceous aerosols, on top of the expected importance of dynamic meteorology. These findings clearly highlight the need to consider AMI in hydrometeorological monitoring, modeling, and reanalyses.

Plain Language Summary

Understanding the changes in snow cover over glaciers in High Mountain Asia (HMA) is important yet challenging. Despite its impact on water resources, physical processes that drive these changes are complex. In particular, large-scale weather patterns, together with aerosol pollution hotspots in the vicinity, and its steep elevation strongly interact with each other. We use a statistical approach to assess the relevance of these interactions using geophysical data from present day reanalysis and observed snow cover extent from satellite products for two decades. We find that during the late snowmelt period from June to July, interactions between aerosols and meteorology are significant, specifically in low snow cover regions. Interactions of individual aerosol species, especially carbonaceous aerosols like black carbon are more important than total aerosol concentration. This approach in quantifying the interactions of these processes can help improve the monitoring and modeling of snow hydrology. Representing these relevant interactions in current models and reanalysis of hydrometeorology can lead to more accurate predictions of the state of snow for critical regions like HMA.

[#] Corresponding Author: Chayan Roychoudhury (croychoudhury@arizona.edu)

Keywords: aerosol-meteorology interactions, ERA5/CAMS-EAC4, snow cover, relative importance, High Mountain Asia

1 Introduction

The High Mountain Asia (HMA) region, often termed as the Third Pole, contains the largest volume of ice outside the poles (Farinotti et al., 2019). Glaciers in HMA provide the hydrological needs of approximately 1.5 billion people via snowmelt and glacial discharge from its major rivers (e.g., Bolch et al., 2012; Pritchard, 2019). As indicators of climate change, glaciers in HMA have been studied through satellite observations to better understand the implications on the water supply in downstream inhabited regions and natural hazards. Snow cover (SC) and its extent is a widely used parameter to characterize the spatiotemporal distribution of these glaciers since it serves as a conduit between surface processes and the atmosphere over it. In fact, observational studies (Notarnicola, 2020) and future projections (Lalande et al., 2021) report that approximately 86% of HMA areal extent exhibit negative trends in SC due to climate change.

Recent studies have attributed this decline to atmospheric teleconnections (e.g., Wang et al., 2021), solar radiation, temperature, precipitation, and their seasonal fluctuations (e.g., Bhattacharya et al., 2021; Johnson & Rupper, 2020; Sahu & Gupta, 2020 and references therein). In addition, there are topographic controls on SC variability and associated runoff due to HMA's steep and complex terrain (Gurung et al., 2017; Jain et al., 2009; She et al., 2015). However, the response of glaciers to climate is not strictly linear and often complex. For example, increase in temperature is followed by snowmelt and decrease in snow albedo (reflectivity) which further continues snowmelt. Decrease in precipitation (that fall as snow) associated with warming maintains this feedback. Although temperature and snowmelt decrease with elevation, glaciers at higher elevations are more susceptible to changes in temperature and precipitation (Pepin et al., 2015; Rangwala & Miller, 2012). Spatial heterogeneity in SC variability is thus a common observation over HMA because of these non-linear processes, which often makes it more difficult to estimate the sensitivity of SC to different climatic factors.

Atmospheric aerosols and their deposition, particularly light absorbing particles (LAPs) like dust and black carbon (BC) also add to the complexity in snow-climate processes by accelerating snowmelt (e.g., He et al., 2014; Lee et al., 2017; Li et al., 2022; Xu et al., 2016). Deposition of LAPs onto snow causes snow darkening which reduces snow albedo and subsequently enhances snowmelt. This continues as the underlying darker surface beneath the snow remains exposed. This aerosol-induced snow albedo effect is identified as one of the primary but highly uncertain agents affecting climate change in addition to greenhouse gases (Shindell and Faluvegi, 2009; Skiles et al., 2018 and references therein). Among LAPs, most studies have placed importance on BC deposition rather than dust, owing to its absorption efficiency and proximity of HMA to regions with strong combustion activities (Bond et al., 2013 and references therein; Das et al., 2022; Gul et al., 2021; Schmale et al., 2017). Other studies, however, report the importance of dust radiative effects on snowmelt, mostly arising from large-scale meteorological transport and high elevation (Hu et al., 2020; Kaspari et al., 2014; Sarangi et al., 2019, 2020). This points to the uncertainty in determining the comparative effects between different LAPs as such studies have been limited by far.

While these studies have elucidated the contribution of both meteorology and aerosols, albeit separately, there is a compelling need to quantify their relative importance and the interactions between different drivers of SC evolution. Here, we analyze the relevance of these factors by conducting a statistical analysis of hydrometeorological variables from the European Centre for Medium-Range Weather Forecasts (ECMWF) reanalysis onto satellite-derived snow cover fraction (SCF) from Moderate Resolution Imaging Spectroradiometer (MODIS). Although these complex interactions can be studied through modeling experiments (e.g., using the Regional Climate Model (RegCM4.6) coupled with Snow, Ice and Aerosol Radiation (SNICAR) (Usha et al., 2022)), such an approach is often computationally expensive and entails rigorous assessment. Instead, we use a multivariate regression method with non-linear interaction terms of reanalysis state variables onto observed SCF to quantify the relative contribution of these interactions. From these analyses, we aim to unravel these interactions that are otherwise already embodied in these observationally constrained models. In Section 2, we described the methodology and datasets used. We discuss our results of our relevance analysis in Section 3 and highlight implications in Section 4.

2 Methodology

2.1 Study Region

A total of 6 glacier regions (GRs) are defined for HMA following the classification in Randolph Glacier Inventory version 6 (Pfeffer et al., 2014). This comprises a total of 15 glacier basins that are aggregated into 6 major GRs for this study. We show in Figure 1a the geographical extent of the glacier basins over HMA. GRs marked in red (blue) denote regions of high snow cover or HSC (low snow-covered or LSC) based on spatiotemporal mean of SCF which ranges from 4% to 20% (1 to 12%) across the most recent 16-year period from 2003 to 2018.

2.2 Data

2.2.1 MODIS Snow Cover (Predictand)

We use daily snow cover fraction (SCF) or extent maps at a spatial resolution of 0.05^{o} as the predictand in our regression analysis. These SCF datasets, which are obtained from the National Snow and Ice Data Center (NSIDC), are satellite derived SCFs based on the Normalized Difference Snow Index (NDSI) (Hall & Riggs, 2007). Specifically, we use MODIS (Terra and Aqua) Daily Level 3 (L3) Global 0.05 Deg Climate Modeling Grid (CMG) Version 6 product with pixels having only recommended quality flags of 0. These products have been used in previous studies where they reported promising results and high accuracy over HMA (Immerzeel et al., 2009; Li et al., 2018; Pu et al., 2007).

2.2.2 ECMWF Reanalyses (MET and AER Predictors)

ERA5. We use select hydrometeorological state variables from ERA5 reanalysis (Hersbach et al., 2020) at a spatial resolution of 0.25° as one group of predictors in our regression. Considering the scarcity of observations across HMA, its remote location and complex terrain, reanalyses such as ERA5, which is a fifth-generation reanalysis from ECMWF, provide a suitable option for long-term study of this region. ERA5 are used for glacier related studies and as atmospheric forcing for regional downscaling efforts (e.g., Arndt et al., 2021; Azam & Srivastava, 2020; Khanal et al., 2021; Sahu & Gupta, 2020). The meteorological variables, defined hereafter as MET, are aggregated from hourly to daily resolution to match MODIS SCF temporal resolution. These MET variables include a) *temperature* (2-m temperature, skin temperature), b) *cloud cover* (total, low, mid, and high-level cloud), c) *dynamic circulation* (mean sea level pressure, geopotential height at 500 hPa and 300 hPa, 10-m zonal and meridional winds), d) *radiation* related surface fluxes (sensible and latent heat), and e) *moisture* (2-m specific humidity, sum of large-scale and convective rain rate). We note that temperature, precipitation, surface radiative fluxes along with cloud cover are considered to be the most important factors in glacier mass balance studies (Armstrong & Brun, 2008; Ohmura et al., 1992; Pepin & Norris, 2005). The dynamic circulation variables are chosen considering the association of wind-driven processes and atmospheric teleconnections on SC (Mott et al., 2018; Yuan et al., 2008). ERA5 uses a single-layer snow model (Dutra et al., 2010), where snow related parameters are calculated using thermodynamic variables to estimate the land surface response to atmospheric forcing. Notably, aerosol related parameterizations are absent in the scheme, which could be relevant given previously described interactions between aerosols and the cryosphere.

CAMS-EAC4. We use the chemical and aerosol reanalysis from Copernicus Atmosphere Monitoring Service (CAMS) ECMWF Atmospheric Composition (EAC4) for aerosol related variables in our predictors. CAMS-EAC4 uses the up-to-date version of the Integrated Forecast System (IFS) and assimilates space-based aerosol optical depths (AOD) including MODIS. CAMS-EAC4 provides 3-hourly 0.75° resolution data which we aggregate into daily data to match MODIS SCF. It uses an aerosol module that simulates major tropospheric aerosol species (Inness et al., 2019). Aerosol variables, defined as AER hereafter, consists of both AOD at 550 nm and surface mass mixing ratios (SMXR) that we grouped according to species; i.e., a) carbonaceous (black carbon or BC and organic matter or OC AOD, hydrophilic and hydrophobic BC and OC SMXR), b) dust (DU) (AOD and the sum of three types of DU SMXRs at three size bins), c) sulphate (SU) (AOD and SMXR), d) others (sea salt or SS AOD and the sum of three types of SS SMXRs at three size bins). Several evaluation studies over HMA and other regions have used CAMS-EAC4 successfully albeit with some biases (e.g., Fu et al., 2022; Gueymard & Yang, 2020)

2.2.3 GMTED 2010 Elevation (ELEV Predictor)

We use the Global Multi-resolution Terrain Elevation Data (GMTED 2010) for the elevation variable as one of our predictors. This is a global digital elevation model with elevation data given at three resolutions: 1000, 500 and 250 m (Danielson & Gesch, 2011) with reported uncertainty of about 4 m over HMA (Carabajal et. al., 2011; Grohmann, 2016). The dataset was downloaded from temis.nl where several coarser resolutions are also available (e.g., 0.75°, 0.50° among others).

SCF, MET and ELEV are regridded to a resolution of 0.75° to match the spatial resolution of AER variables. Figure 1 shows the spatial distribution of multi-year averaged SCF and key relevant meteorology and aerosol variables over HMA. We see an overestimation of SCF in ERA5 (Figure 1b) compared to MODIS SCF. The large positive bias for ERA5 SCF has been observed in a previous study which has been attributed to excessive snowfall (Orsolini et al., 2019). The mean spatial patterns of these meteorological and aerosol variables qualitatively reflect the non-linear relationships between SCF, MET, and AER which we will further quantify in our regression analysis.

2.3 Relative Importance Analysis

For each GR, a multiple linear regression (MLR) model of daily 0.75° MODIS SCF for each month across all years (2003-2018) is formulated using AER, MET, and ELEV as predictors. We also considered second-order product interaction terms between AER, MET, and ELEV to account for non-linear relationships between these geophysical variables and SCF (Cortina, 1993; Jaccard et al., 1990). A similar approach on using second-order terms is used in previous studies by Ho Park et al. (2021) and Guo et. al. (2014). The MLR model is expressed in Equation 1 as:

$$y \approx \sum_{i=1}^{27} \alpha_i x_i + \sum_{j=28}^{378} \alpha_j x_i x_{i'} \tag{1}$$

where y is the standardized daily MODIS SCF, x_i are the standardized predictor variables, and $x_i x_{i'}$ are the two-way product interaction terms using the standardized values of x_i. Standardization refers to rescaling a variable to a mean of 0 and a standard deviation of 1. The partial coefficients α_1...., α_{378} represent the relative importance of each term in the MLR model. The first 27 terms on the right-hand side of Equation 1 comprise of *main effects* depicted by the individual AER, MET, and ELEV variables while the rest of 351 terms consist of *interaction effects* shown as product terms among the individual predictors. We then classify the interaction terms into 5 groups: 1) AER-AER (between speciated AOD and SMXR), 2) AER-MET (between aerosol and meteorological variables), 3) AER-ELEV (between elevation and aerosol variables), 4) MET-ELEV (between elevation and meteorological variables), and 5) MET-MET (between meteorological variables themselves).

We use the relative importance (RI) analysis introduced by Johnson (2000) and further described by Tonidandel & LeBreton (2011) to minimize multi-collinearity between the explanatory variables. This algorithm quantifies the proportion of the explained variance in SCF. The relative importance or weight is estimated by transforming the original predictors to their orthogonal equivalent before calculating the regression coefficients. Each relative weight is interpreted to be the independent contribution of the predictor terms as a fraction of the explained variance in SCF. Details of the algorithm are provided in Supplementary Information. Finally, we implement a bootstrapping procedure with 1000 iterations as suggested by Efron & Tibshirani (1986) to estimate confidence intervals for these weights.

3 Results and Discussions

Figure 2a shows the seasonality of SCF for both HSC and LSC regions, where HSC regions show a higher degree of SCF variability with an interquartile range (IQR) of 9% while LSC regions have lower variability (IQR of 4%). The results of the monthly RI analysis of the predictors and their interactions for HSC and LSC regions are shown in Figure 2b-j. We grouped the relative weights of predictors from the monthly MLR models based on their interactions (defined in Section 2.2). Aerosol interactions with meteorology (AMI) are grouped as AER-MET + AER-AER + AER while sole meteorology interactions are defined as MET-MET + MET. Interactions with elevation were treated separately. For LSC regions, RI of AMI shows a statistically significant 7% increase from June to July as seen in Figure 2d, compared to HSC regions where the RI remains relatively stable for all months. Meteorology interactions for LSC regions show a corresponding statistically significant 13% decrease in RI from June to July. The period of May to June over HMA is attributed to accelerated snowmelt along with high aerosol loading. The increase in AMI during the late snowmelt period (June-July) is consistent with studies demonstrating the radiative impact of LAPs that in turn increase tropospheric temperature inducing convection, moisture transport, and cloud formation over the Himalayas and the Tibetan Plateau (Lau et al., 2010; Sharma et al., 2022; Usha et al., 2020). Elevation related interactions show higher degree of variability in their relevance for both HSC and LSC regions which are dominated by elevation interactions with meteorology (MET-ELEV) with a maximum of 20% in RI (Figure 2g-j). While AER-ELEV interactions are relatively negligible, its monthly variability in RI for HSC regions is significant. We note that there is increasing evidence of amplified warming with elevation in mountainous regions of HMA that supports our results (Dimri et al., 2022; Ghatak et al., 2014; Guo et al., 2021; Li et al., 2020). Complex processes between cloud cover, radiation, and moisture as well as aerosols at higher elevations have also been associated with elevation dependent warming. Carbonaceous aerosols like BC have prominent snowmelt effects at lower elevations, while dust-induced snowmelt dominates at higher elevations (Sarangi et al., 2020; Xu et al., 2016).

We then performed a series of sensitivity tests (as described in Table S1) by eliminating certain variables from each MLR model and comparing the RI of interactions in LSC regions with the "control" model results shown in Figure 2. Monthly RI of AMI are shown in Figure 3a. Cases 2-4 show a maximum of 24% decrease in RI compared to Cases 0 and 1. The characteristic peak in aerosol interactions as observed in Figure 2c-d during June and July are not noticeable when interaction terms containing individual aerosol species are removed (Case 2). This clearly suggests that species-related interactions are more relevant for SC variability in LSC regions than interactions related to total aerosol loading. Except Case 2, the characteristic peak is still observed for AMI. This confirms the significance of the increase in RI of aerosols for SC variability during late snow melt season. For meteorology related interactions, elevation appears to play an important role as observed in Case 1 of Figure 3b. Removing elevation from the MLR model decreases the RI of meteorology interactions by up to 19% suggesting the high sensitivity of SC variability to MET-ELEV interactions. As previously described, past studies have pointed out the sensitivity of SC to elevation over HMA in addition to trends in temperature and precipitation, which is consistent with our findings (Jain et al., 2009; Li et al., 2018; Rangwala & Miller, 2012; She et al., 2015; Wang et al., 2019). For HSC regions, our sensitivity tests show similar results as to LSC regions but with no significant change in RI of aerosol or meteorology interactions, confirming the sensitivity of aerosol and meteorology related interactions in LSC regions.

We present in Figure 4 the decomposition of the aerosol and meteorology related interactions for LSC regions into different predictor types. Among aerosol related interactions, we find that the RI of carbonaceous aerosols is the highest across all months with the characteristic peak in the late snowmelt season as observed in Figure 2. In addition, carbonaceous aerosols show the highest month-to-month variability of maximum 6% in RI compared to other aerosol types (Figure 4b). During this period, carbonaceous aerosols show the maximum rise (3%) in RI. A possible explanation could be that carbonaceous aerosols are particularly high in abundance from April to May (pre-monsoon) over South and East Asian regions surrounding HMA, which could lead to significant interactions with meteorology in June to July (Das et al., 2022; Kumar et al., 2011; Lau et al., 2006; Zhao et al., 2017). Specifically, Zhao et al. (2017) reported high BC loading during pre-monsoon over the Tibetan Plateau. Springtime crop-residue burning in northern India has also been shown to increase black carbon and AOD levels in the central Himalayas by ~145% and ~150%, respectively (Kumar et al., 2011). Among meteorological interactions shown in Figure 4a, we see that circulation related variables have the highest RI followed by cloud cover and temperature, with the characteristic dip in RI during late snow melt (June and July). Thus, interactions related to circulation contribute significantly to the SC variability in LSC regions followed by cloud cover and temperature. Circulation related variables account for large-scale atmospheric dynamics that can influence the surface energy budget and snow mass balance. We hypothesize that dynamical variables contribute to the relatively higher importance across all months, as studies have reported the possible relationships between glaciers in HMA and the relevant atmospheric teleconnections that influence the Asian monsoon system (Arndt et al., 2021; Forsythe et al., 2017; Priya et al., 2017; Wu et al., 2012; Yuan et al., 2008; Zhao et al., 2007).

4 Summary and Implications

We estimated the monthly relative importance (RI) of AER and MET interactions (AMI) from ECMWF reanalyses in driving MODIS SC over six HMA glacier regions. We find that snow cover fraction is particularly sensitive to AMI during snowmelt period, especially in low snow-covered (LSC) regions. MET interactions on the other hand exclusively dominate the RI for SC variability in both high (HSC) and LSC regions. We also find that the interactions related to carbonaceous aerosols are the highest in their relevance to SC compared to other aerosol species like dust. More importantly, our sensitivity tests show that species-related interactions matter more than the total aerosol loading in association to SC variability, while MET-ELEV interactions matter more during snowmelt season. These findings appear to be very consistent with literature. Albeit simplified relative to machine/deep learning (ML/DL) approaches, this RI estimation using interaction terms offers a useful and explainable diagnostic tool in unraveling complex non-linear interactions that could otherwise be quantified through more expensive global sensitivity analyses using Earth system models (ESM). Our results on the importance of AMI during snowmelt highlights the need to: 1) improve observing system on snow hydrology in this region by augmenting with in-situ and remotely sensed aerosol and meteorological monitoring; and 2) represent these interactions in coupled ESMs and reanalyses like ERA5 to improve the predictive capability of snow hydrology. While this study only examines interactions embodied in ERA5/CAMS-EAC4, we view this to be a useful starting point in unfolding non-linear interactions in ESMs. We note however that future studies on associating these interactions with snow albedo, snow depth or snow water equivalent, as well as investigating other modeling/reanalysis systems like NASA MERRA-2 are essential to corroborate our findings. Application of promising ML/DL algorithms on estimating relevance should also be considered.

Acknowledgments

This work is supported by a NASA HiMAT2 grant (#NNH19ZDA001N). We acknowledge the National Center for Atmospheric Research (NCAR) (sponsored by the National Science Foundation (NSF)) for this ongoing work. HiMAT2 is an interdisciplinary effort to understand the cryospheric and hydrological state of HMA. This work is in tandem with the goals of the Aerosol subgroup under HiMAT2 that seeks to quantify the deposition of aerosols over snow in HMA.

Open Research

Data Availability Statement

MODIS Level 3 Snow Cover Products available at https://nsidc.org/data/MOD10C1/versions/61 and https://nsidc.org/data/MYD10C1/versions/61 for registered users at Earthdata (https://urs.earthdata.nasa.gov/).

ERA5 hourly data available at the Copernicus Climate Data Store for registered users to download. Hourly data for single levels can be found at https://cds.climate.copernicus.eu/cdsapp#!/dataset/reanalysis-era5-single-levels?tab=overview

Hourly data for pressure levels can be found at https://cds.climate.copernicus.eu/cdsapp#!/dataset/reanalysis-era5-pressure-levels?tab=overview

CAMS-EAC4 3 hourly reanalysis data from ECMWF is available at the Copernicus Atmospheric Data Store from https://ads.atmosphere.copernicus.eu/cdsapp#!/dataset/cams-global-reanalysis-eac4?tab=overview (requires registration as well).

GMTED2010 global elevation data available at various resolutions from https://www.temis.nl/data/gmted2010/

References

Armstrong, R. L., & Brun, E. (2008). *Snow and climate: physical processes, surface energy exchange and modeling*. Cambridge University Press.

Arndt, A., Scherer, D., & Schneider, C. (2021). Atmosphere Driven Mass-Balance Sensitivity of Halji Glacier, Himalayas. *Atmosphere*, *12*(4), 426. https://doi.org/10.3390/atmos12040426

Azam, Mohd. F., & Srivastava, S. (2020). Mass balance and runoff modelling of partially debris-covered Dokriani Glacier in monsoon-dominated Himalaya using ERA5 data since 1979. *Journal of Hydrology*, *590*, 125432. https://doi.org/10.1016/j.jhydrol.2020.125432

Bhattacharya, A., Bolch, T., Mukherjee, K., King, O., Menounos, B., Kapitsa, V., et al. (2021). High Mountain Asian glacier response to climate revealed by multi-temporal satellite observations since the 1960s. *Nature Communications*, *12*(1), 4133. https://doi.org/10.1038/s41467-021-24180-y

Bolch, T., Kulkarni, A., Kääb, A., Huggel, C., Paul, F., Cogley, J. G., et al. (2012). The State and Fate of Himalayan Glaciers. *Science*, *336*(6079), 310–314. https://doi.org/10.1126/science.1215828

Bond, T. C., Doherty, S. J., Fahey, D. W., Forster, P. M., Berntsen, T., DeAngelo, B. J., et al. (2013). Bounding the role of black carbon in the climate system: A scientific assessment. *Journal of Geophysical Research: Atmospheres*, *118*(11), 5380–5552. https://doi.org/10.1002/jgrd.50171

Carabajal, C. C., Harding, D. J., Boy, J.-P., Danielson, J. J., Gesch, D. B., & Suchdeo, V. P. (2011). Evaluation of the Global Multi-Resolution Terrain Elevation Data 2010 (GMTED2010) using ICESat geodetic control. In *International Symposium on Lidar and Radar Mapping 2011: Technologies and Applications* (Vol. 8286, pp. 532–544). SPIE. https://doi.org/10.1117/12.912776

Cortina, J. M. (1993). Interaction, nonlinearity, and multicollinearity: Implications for multiple regression. *Journal of Management*, *19*(4), 915–922. https://doi.org/10.1016/0149-2063(93)90035-L

Danielson, J. J., & Gesch, D. B. (2011). *Global multi-resolution terrain elevation data 2010 (GMTED2010)*. US Department of the Interior, US Geological Survey Washington, DC, USA.

Das, S., Giorgi, F., Coppola, E., Panicker, A. S., Gautam, A. S., Nair, V. S., & Giuliani, G. (2022). Linkage between the absorbing aerosol-induced snow darkening effects over the Himalayas-Tibetan Plateau and the pre-monsoon climate over northern India. *Theoretical and Applied Climatology*, *147*(3), 1033–1048. https://doi.org/10.1007/s00704-021-03871-y

Dimri, A. P., Palazzi, E., & Daloz, A. S. (2022). Elevation dependent precipitation and temperature changes over Indian Himalayan region. *Climate Dynamics*. https://doi.org/10.1007/s00382-021-06113-z

Dutra, E., Balsamo, G., Viterbo, P., Miranda, P. M. A., Beljaars, A., Schär, C., & Elder, K. (2010). An Improved Snow Scheme for the ECMWF Land Surface Model: Description and Offline Validation. *Journal of Hydrometeorology*, *11*(4), 899–916. https://doi.org/10.1175/2010JHM1249.1

Efron, B., & Tibshirani, R. (1986). Bootstrap methods for standard errors, confidence intervals, and other measures of statistical accuracy. *Statistical Science*, 54–75.

Farinotti, D., Huss, M., Fürst, J. J., Landmann, J., Machguth, H., Maussion, F., & Pandit, A. (2019). A consensus estimate for the ice thickness distribution of all glaciers on Earth. *Nature Geoscience*, *12*, 168–173. https://doi.org/10.1038/s41561-019-0300-3

Forsythe, N., Fowler, H. J., Li, X.-F., Blenkinsop, S., & Pritchard, D. (2017). Karakoram temperature and glacial melt driven by regional atmospheric circulation variability. *Nature Climate Change*, *7*(9), 664–670. https://doi.org/10.1038/nclimate3361

Fu, D., Liu, M., Yang, D., Che, H., & Xia, X. (2022). Influences of atmospheric reanalysis on the accuracy of clear-sky irradiance estimates: Comparing MERRA-2 and CAMS. *Atmospheric Environment*, *277*, 119080. https://doi.org/10.1016/j.atmosenv.2022.119080

Ghatak, D., Sinsky, E., & Miller, J. (2014). Role of snow-albedo feedback in higher elevation warming over the Himalayas, Tibetan Plateau and Central Asia. *Environmental Research Letters*, *9*(11), 114008. https://doi.org/10.1088/1748-9326/9/11/114008

Grohmann, C. H. (2016). COMPARATIVE ANALYSIS OF GLOBAL DIGITAL ELEVATION MODELS AND ULTRA-PROMINENT MOUNTAIN PEAKS. *ISPRS Annals of Photogrammetry, Remote Sensing and Spatial Information Sciences*, *III–4*, 17–23. https://doi.org/10.5194/isprsannals-III-4-17-2016

Gueymard, C. A., & Yang, D. (2020). Worldwide validation of CAMS and MERRA-2 reanalysis aerosol optical depth products using 15 years of AERONET observations. *Atmospheric Environment*, *225*, 117216. https://doi.org/10.1016/j.atmosenv.2019.117216

Gul, C., Mahapatra, P. S., Kang, S., Singh, P. K., Wu, X., He, C., et al. (2021). Black carbon concentration in the central Himalayas: Impact on glacier melt and potential source contribution. *Environmental Pollution*, *275*, 116544. https://doi.org/10.1016/j.envpol.2021.116544

Guo, D., Pepin, N., Yang, K., Sun, J., & Li, D. (2021). Local changes in snow depth dominate the evolving pattern of elevation-dependent warming on the Tibetan Plateau. *Science Bulletin*, *66*(11), 1146–1150. https://doi.org/10.1016/j.scib.2021.02.013

Guo, Z., Wang, M., Qian, Y., Larson, V. E., Ghan, S., Ovchinnikov, M., et al. (2014). A sensitivity analysis of cloud properties to CLUBB parameters in the single-column Community Atmosphere Model (SCAM5). *Journal of Advances in Modeling Earth Systems*, *6*(3), 829–858. https://doi.org/10.1002/2014MS000315

Gurung, D. R., Maharjan, S. B., Shrestha, A. B., Shrestha, M. S., Bajracharya, S. R., & Murthy, M. S. R. (2017). Climate and topographic controls on snow cover dynamics in the Hindu Kush Himalaya. *International Journal of Climatology*, *37*(10), 3873–3882. https://doi.org/10.1002/joc.4961

Hall, D. K., & Riggs, G. A. (2007). Accuracy assessment of the MODIS snow products. *Hydrological Processes*, *21*(12), 1534–1547. https://doi.org/10.1002/hyp.6715

He, C., Li, Q., Liou, K.-N., Takano, Y., Gu, Y., Qi, L., et al. (2014). Black carbon radiative forcing over the Tibetan Plateau. *Geophysical Research Letters*, *41*(22), 7806–7813. https://doi.org/10.1002/2014GL062191

Hersbach, H., Bell, B., Berrisford, P., Hirahara, S., Horányi, A., Muñoz-Sabater, J., et al. (2020). The ERA5 global reanalysis. *Quarterly Journal of the Royal Meteorological Society*, *146*(730), 1999–2049. https://doi.org/10.1002/qj.3803

Ho Park, M., Ju, M., Jeong, S., & Young Kim, J. (2021). Incorporating interaction terms in multivariate linear regression for post-event flood waste estimation. *Waste Management*, *124*, 377–384. https://doi.org/10.1016/j.wasman.2021.02.004

Hu, Z., Kang, S., Li, X., Li, C., & Sillanpää, M. (2020). Relative contribution of mineral dust versus black carbon to Third Pole glacier melting. *Atmospheric Environment*, *223*, 117288. https://doi.org/10.1016/j.atmosenv.2020.117288

Immerzeel, W. W., Droogers, P., de Jong, S. M., & Bierkens, M. F. P. (2009). Large-scale monitoring of snow cover and runoff simulation in Himalayan river basins using remote sensing. *Remote Sensing of Environment*, *113*(1), 40–49. https://doi.org/10.1016/j.rse.2008.08.010

Inness, A., Ades, M., Agustí-Panareda, A., Barré, J., Benedictow, A., Blechschmidt, A.-M., et al. (2019). The CAMS reanalysis of atmospheric composition. *Atmospheric Chemistry and Physics*, *19*(6), 3515–3556. https://doi.org/10.5194/acp-19-3515-2019

Jaccard, J., Wan, C. K., & Turrisi, R. (1990). The Detection and Interpretation of Interaction Effects Between Continuous Variables in Multiple Regression. *Multivariate Behavioral Research*, *25*(4), 467–478. https://doi.org/10.1207/s15327906mbr2504_4

Jain, S. K., Goswami, A., & Saraf, A. K. (2009). Role of Elevation and Aspect in Snow Distribution in Western Himalaya. *Water Resources Management*, *23*(1), 71–83. https://doi.org/10.1007/s11269-008-9265-5

Johnson, E., & Rupper, S. (2020). An Examination of Physical Processes That Trigger the Albedo-Feedback on Glacier Surfaces and Implications for Regional Glacier Mass Balance Across High Mountain Asia. *Frontiers in Earth Science*, *8*, 129. https://doi.org/10.3389/feart.2020.00129

Johnson, J. W. (2000). A heuristic method for estimating the relative weight of predictor variables in multiple regression. *Multivariate Behavioral Research*, *35*(1), 1–19. https://doi.org/10.1207/S15327906MBR3501_1

Kaspari, S., Painter, T. H., Gysel, M., Skiles, S. M., & Schwikowski, M. (2014). Seasonal and elevational variations of black carbon and dust in snow and ice in the Solu-Khumbu, Nepal and estimated radiative forcings. *Atmospheric Chemistry and Physics*, *14*(15), 8089–8103. https://doi.org/10.5194/acp-14-8089-2014

Khanal, S., Lutz, A. f., Kraaijenbrink, P. D. A., van den Hurk, B., Yao, T., & Immerzeel, W. W. (2021). Variable 21st Century Climate Change Response for Rivers in High Mountain Asia at Seasonal to Decadal Time Scales. *Water Resources Research*, *57*(5), e2020WR029266. https://doi.org/10.1029/2020WR029266

Kumar, R., Naja, M., Satheesh, S. K., Ojha, N., Joshi, H., Sarangi, T., et al. (2011). Influences of the springtime northern Indian biomass burning over the central Himalayas. *Journal of Geophysical Research: Atmospheres*, *116*(D19). https://doi.org/10.1029/2010JD015509

Lalande, M., Ménégoz, M., Krinner, G., Naegeli, K., & Wunderle, S. (2021). Climate change in the High Mountain Asia in CMIP6. *Earth System Dynamics*, *12*(4), 1061–1098. https://doi.org/10.5194/esd-12-1061-2021

Lau, K. M., Kim, M. K., & Kim, K. M. (2006). Asian summer monsoon anomalies induced by aerosol direct forcing: the role of the Tibetan Plateau. *Climate Dynamics*, *26*(7), 855–864. https://doi.org/10.1007/s00382-006-0114-z

Lau, W. K. M., Kim, M.-K., Kim, K. M., & Lee, W. S. (2010). Enhanced surface warming and accelerated snow melt in the Himalayas and Tibetan Plateau induced by absorbing aerosols. *Environmental Research Letters*, *5*(2), 025204. https://doi.org/10.1088/1748-9326/5/2/025204

Lee, W. L., Liou, K. N., He, C., Liang, H. C., Wang, T.-C., Li, Q., et al. (2017). Impact of absorbing aerosol deposition on snow albedo reduction over the southern Tibetan plateau based on satellite observations. *Theoretical and Applied Climatology*, *129*(3), 1373–1382. https://doi.org/10.1007/s00704-016-1860-4

Li, B., Chen, Y., & Shi, X. (2020). Does elevation dependent warming exist in high mountain Asia? *Environmental Research Letters*, *15*(2), 024012. https://doi.org/10.1088/1748-9326/ab6d7f

Li, C, Yan, F., Zhang, C., Kang, S., Rai, M., Zhang, H., et al. (2022). Coupling of decreased snow accumulation and increased light-absorbing particles accelerates glacier retreat in the Tibetan Plateau. *Science of The Total Environment*, *809*, 151095. https://doi.org/10.1016/j.scitotenv.2021.151095

Li, C, Su, F., Yang, D., Tong, K., Meng, F., & Kan, B. (2018). Spatiotemporal variation of snow cover over the Tibetan Plateau based on MODIS snow product, 2001–2014. *International Journal of Climatology*, *38*(2), 708–728. https://doi.org/10.1002/joc.5204

Mott, R., Vionnet, V., & Grünewald, T. (2018). The Seasonal Snow Cover Dynamics: Review on Wind-Driven Coupling Processes. *Frontiers in Earth Science*, *6*. Retrieved from https://www.frontiersin.org/article/10.3389/feart.2018.00197

Notarnicola, C. (2020). Observing Snow Cover and Water Resource Changes in the High Mountain Asia Region in Comparison with Global Mountain Trends over 2000–2018. *Remote Sensing*, *12*(23), 3913. https://doi.org/10.3390/rs12233913

Ohmura, A., Kasser, P., & Funk, M. (1992). Climate at the Equilibrium Line of Glaciers. *Journal of Glaciology*, *38*(130), 397–411. https://doi.org/10.3189/S0022143000002276

Orsolini, Y., Wegmann, M., Dutra, E., Liu, B., Balsamo, G., Yang, K., et al. (2019). Evaluation of snow depth and snow cover over the Tibetan Plateau in global reanalyses using in situ and satellite remote sensing observations. *The Cryosphere*, *13*(8), 2221–2239. https://doi.org/10.5194/tc-13-2221-2019

Pepin, N., Bradley, R. S., Diaz, H. F., Baraer, M., Caceres, E. B., Forsythe, N., et al. (2015). Elevation-dependent warming in mountain regions of the world. *Nature Climate Change*, *5*(5), 424–430. https://doi.org/10.1038/nclimate2563

Pepin, N. C., & Norris, J. R. (2005). An examination of the differences between surface and free-air temperature trend at high-elevation sites: Relationships with cloud cover, snow cover, and wind. *Journal of Geophysical Research: Atmospheres*, *110*(D24). https://doi.org/10.1029/2005JD006150

Pfeffer, W. T., Arendt, A. A., Bliss, A., Bolch, T., Cogley, J. G., Gardner, A. S., et al. (2014). The Randolph Glacier Inventory: a globally complete inventory of glaciers. *Journal of Glaciology*, *60*(221), 537–552. https://doi.org/10.3189/2014JoG13J176

Pritchard, H. D. (2019). Asia's shrinking glaciers protect large populations from drought stress. *Nature*, *569*(7758), 649–654. https://doi.org/10.1038/s41586-019-1240-1

Priya, P., Krishnan, R., Mujumdar, M., & Houze, R. A. (2017). Changing monsoon and midlatitude circulation interactions over the Western Himalayas and possible links to occurrences of extreme precipitation. *Climate Dynamics*, *49*(7), 2351–2364. https://doi.org/10.1007/s00382-016-3458-z

Pu, Z., Xu, L., & Salomonson, V. V. (2007). MODIS/Terra observed seasonal variations of snow cover over the Tibetan Plateau. *Geophysical Research Letters*, *34*(6). https://doi.org/10.1029/2007GL029262

Rangwala, I., & Miller, J. R. (2012). Climate change in mountains: a review of elevation-dependent warming and its possible causes. *Climatic Change*, *114*(3), 527–547. https://doi.org/10.1007/s10584-012-0419-3

Sahu, R., & Gupta, R. D. (2020). Snow cover area analysis and its relation with climate variability in Chandra basin, Western Himalaya, during 2001–2017 using MODIS and ERA5 data. *Environmental Monitoring and Assessment*, *192*(8), 489. https://doi.org/10.1007/s10661-020-08442-8

Sarangi, C., Qian, Y., Rittger, K., Bormann, K. J., Liu, Y., Wang, H., et al. (2019). Impact of light-absorbing particles on snow albedo darkening and associated radiative forcing over high-mountain Asia: high-resolution WRF-Chem modeling and new satellite observations. *Atmospheric Chemistry and Physics*, *19*(10), 7105–7128. https://doi.org/10.5194/acp-19-7105-2019

Sarangi, C., Qian, Y., Rittger, K., Ruby Leung, L., Chand, D., Bormann, K. J., & Painter, T. H. (2020). Dust dominates high-altitude snow darkening and melt over high-mountain Asia. *Nature Climate Change*, *10*(11), 1045–1051. https://doi.org/10.1038/s41558-020-00909-3

Schmale, J., Flanner, M., Kang, S., Sprenger, M., Zhang, Q., Guo, J., et al. (2017). Modulation of snow reflectance and snowmelt from Central Asian glaciers by anthropogenic black carbon. *Scientific Reports*, *7*(1), 40501. https://doi.org/10.1038/srep40501

Sharma, A., Bhattacharya, A., & Venkataraman, C. (2022). Influence of aerosol radiative effects on surface temperature and snow melt in the Himalayan region. *Science of The Total Environment*, *810*, 151299. https://doi.org/10.1016/j.scitotenv.2021.151299

She, J., Zhang, Y., Li, X., & Feng, X. (2015). Spatial and Temporal Characteristics of Snow Cover in the Tizinafu Watershed of the Western Kunlun Mountains. *Remote Sensing*, *7*(4), 3426–3445. https://doi.org/10.3390/rs70403426

Shindell, D., & Faluvegi, G. (2009). Climate response to regional radiative forcing during the twentieth century. *Nature Geoscience*, *2*(4), 294–300. https://doi.org/10.1038/ngeo473

Skiles, S. M., Flanner, M., Cook, J. M., Dumont, M., & Painter, T. H. (2018). Radiative forcing by light-absorbing particles in snow. *Nature Climate Change*, *8*(11), 964–971. https://doi.org/10.1038/s41558-018-0296-5

Tonidandel, S., & LeBreton, J. M. (2011). Relative Importance Analysis: A Useful Supplement to Regression Analysis. *Journal of Business and Psychology*, *26*(1), 1–9. https://doi.org/10.1007/s10869-010-9204-3

Usha, K. H., Nair, V. S., & Babu, S. S. (2020). Modeling of aerosol induced snow albedo feedbacks over the Himalayas and its implications on regional climate. *Climate Dynamics*, *54*(9), 4191–4210. https://doi.org/10.1007/s00382-020-05222-5

Usha, K. H., Nair, V. S., & Babu, S. S. (2022). Effects of Aerosol–Induced Snow Albedo Feedback on the Seasonal Snowmelt Over the Himalayan Region. *Water Resources Research*, *58*(2), e2021WR030140. https://doi.org/10.1029/2021WR030140

Wang, R., Liu, S., Shangguan, D., Radić, V., & Zhang, Y. (2019). Spatial Heterogeneity in Glacier Mass-Balance Sensitivity across High Mountain Asia. *Water*, *11*(4), 776. https://doi.org/10.3390/w11040776

Wang, Z., Wu, R., Yang, S., & Lu, M. (2021). An interdecadal change in the influence of ENSO on the spring Tibetan Plateau snow cover variability in the early 2000s. *Journal of Climate*, *1*(aop), 1–1. https://doi.org/10.1175/JCLI-D-21-0348.1

Wu, Z., Li, J., Jiang, Z., & Ma, T. (2012). Modulation of the Tibetan Plateau Snow Cover on the ENSO Teleconnections: From the East Asian Summer Monsoon Perspective. *Journal of Climate*, *25*(7), 2481–2489. https://doi.org/10.1175/JCLI-D-11-00135.1

Xu, Y., Ramanathan, V., & Washington, W. M. (2016). Observed high-altitude warming and snow cover retreat over Tibet and the Himalayas enhanced by black carbon aerosols. *Atmospheric Chemistry and Physics*, *16*(3), 1303–1315. https://doi.org/10.5194/acp-16-1303-2016

Yuan, C., Tozuka, T., Miyasaka, T., & Yamagata, T. (2008). Respective influences of IOD and ENSO on the Tibetan snow cover in early winter. *Climate Dynamics*, *33*(4), 509. https://doi.org/10.1007/s00382-008-0495-2

Zhao, P., Zhou, Z., & Liu, J. (2007). Variability of Tibetan Spring Snow and Its Associations with the Hemispheric Extratropical Circulation and East Asian Summer Monsoon Rainfall: An Observational Investigation. *Journal of Climate*, *20*(15), 3942–3955. https://doi.org/10.1175/JCLI4205.1

Zhao, Z., Wang, Q., Xu, B., Shen, Z., Huang, R., Zhu, C., et al. (2017). Black carbon aerosol and its radiative impact at a high-altitude remote site on the southeastern Tibet Plateau. *Journal of Geophysical Research: Atmospheres*, *122*(10), 5515–5530. https://doi.org/10.1002/2016JD026032

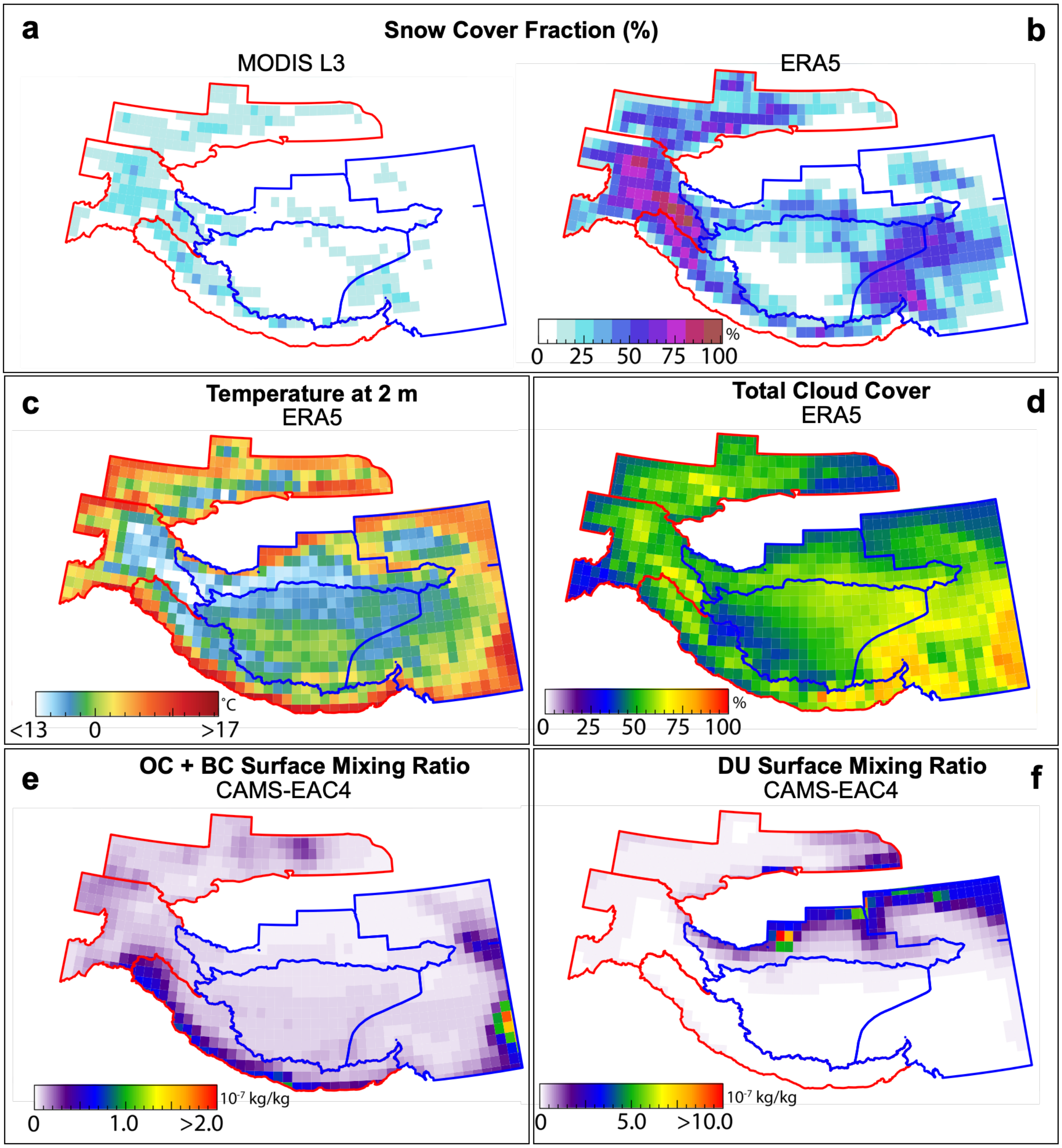

Figure 1. Time average (2003-2018) of daily geophysical products over HMA with geographical outlines from RGI v6. (a and b): snow cover fraction from MODIS Level 3 data and ERA5 reanalysis, respectively. Regions marked in red denote high snow cover (HSC) regions while those in blue denote low snow cover (LSC) regions. (c and d): 2-m temperature and total cloud cover fraction from ERA5 reanalysis. (e): sum of organic matter and black carbon surface mass mixing ratios from CAMS-EAC4 reanalysis. (f): dust surface mass mixing ratios from CAMS-EAC4 reanalysis.

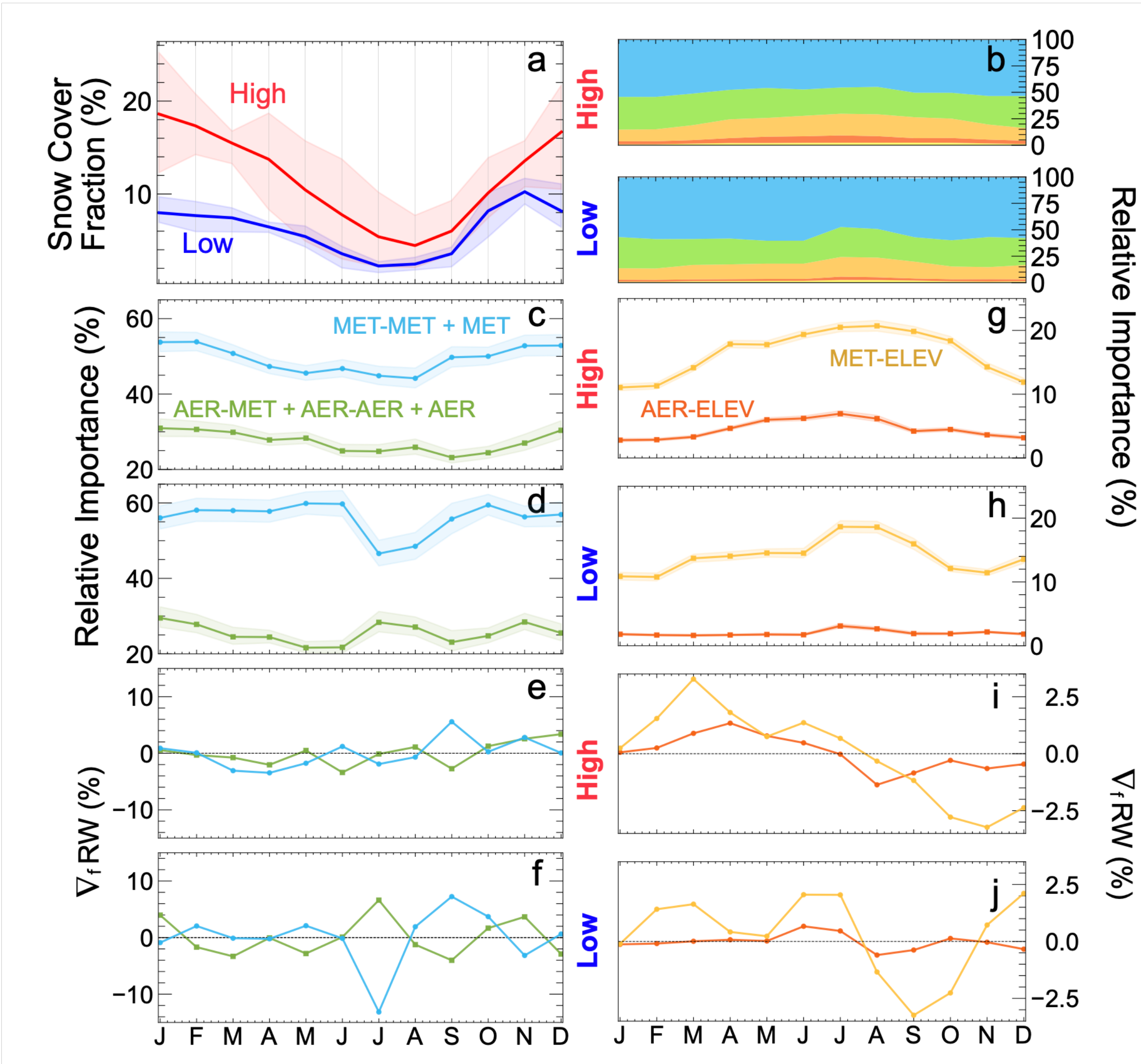

Figure 2. (a): Snow cover fraction averaged over high and low snow-covered (HSC and LSC) regions for each month. The shaded regions refer to the range of monthly snow cover for both HSC and LSC regions. (b): Monthly relative importance (RI) of different groups of interactions (MET-MET+MET in green, AER+AER-AER+AER-MET in blue, MET-ELEV in orange and AER-ELEV in red). RI for elevation (ELEV) not shown as it is negligible. (c-d): Monthly RI of aerosol (green) and meteorology (blue) interactions over high and low snow-covered regions. (e-f): Gradient of monthly relevance for aerosol and meteorology interactions. (e-h): Monthly RI of aerosol (red) and meteorology (orange) interactions with meteorology. (i-j): Gradient of monthly RI of elevation interactions. Shaded regions show the interquartile range (75th to 25th percentile) of RI based on 1000 bootstrap iterations. The gradient for a particular month is based on a forward difference between that month and the prior month.

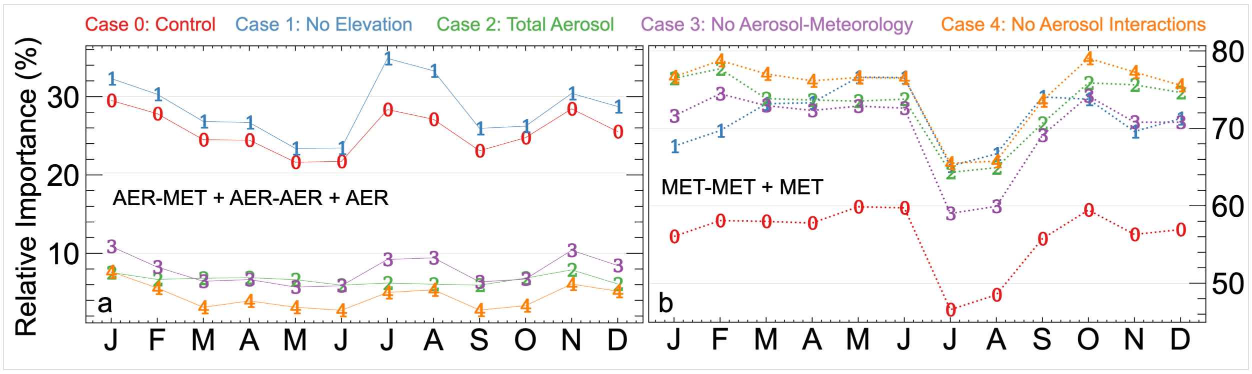

Figure 3. Monthly relative importance (RI) of aerosol (a) and meteorology (b) interactions for different sensitivity tests outlined in Table S1.

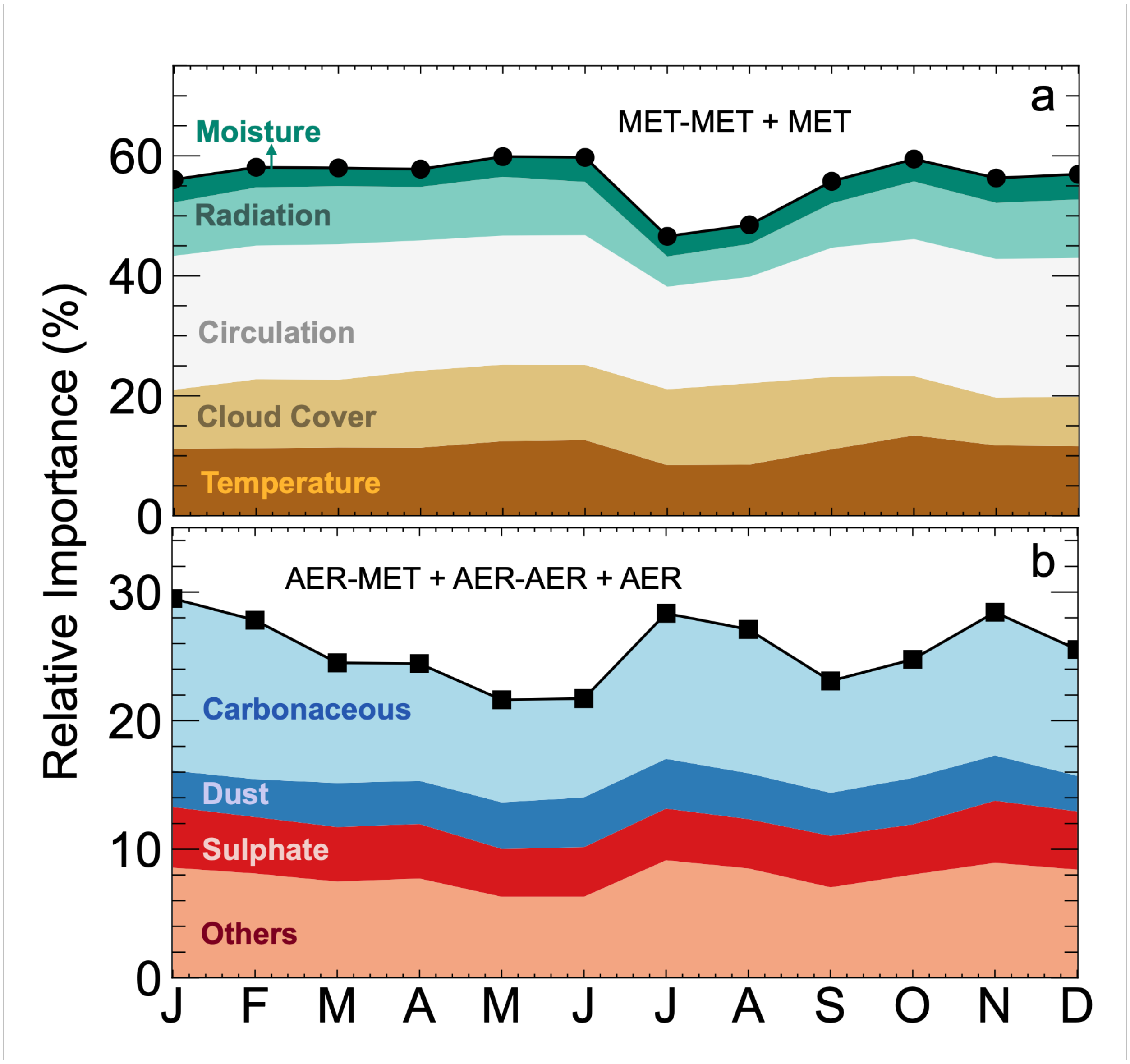

Figure 4. Monthly relative importance (RI) for meteorology (a) and aerosol (b) interactions decomposed to different types of variables outlined in Section 2 (Data).